Atmos. Chem. Phys. Discuss., 12, 20135–20180, 2012
www.atmos-chem-phys-discuss.net/12/20135/2012/
doi:10.5194/acpd-12-20135-2012

Atmospheric Chemistry and Physics Discussions

Hourly elemental concentrations in $PM_{2.5}$ aerosols sampled simultaneously at urban background and road site

M. Dall'Osto[1], X. Querol[1], F. Amato[2], A. Karanasiou[3], F. Lucarelli[4], S. Nava[4], G. Calzolai[4], and M. Chiari[4]

[1]Institute of Environmental Assessment and Water Research, Spanish Research Council (IDAEA-CSIC), c/Jordi Girona 18–26, 08034 Barcelona, Spain
[2]TNO, Built Environment and Geosciences, Dept. of Air Quality and Climate, Utrecht, The Netherlands
[3]Centre for Research in Environmental Epidemiology (CREAL), Barcelona, Spain
[4]National Institute of Nuclear Physics (INFN) and Physics Department, University of Florence, via Sansone 1, 50019 Sesto Fiorentino, Italy

Received: 30 July 2012 – Accepted: 2 August 2012 – Published: 13 August 2012

Correspondence to: M. Dall'Osto (manuel.dallosto@gmail.com)

Published by Copernicus Publications on behalf of the European Geosciences Union.

Abstract

Hourly-resolved aerosol chemical speciation data can be a highly powerful tool to determine the source origin of atmospheric pollutants in urban Environments. Aerosol mass concentrations of seventeen elements (Na, Mg, Al, S, Cl, K, Ca, Ti, V, Cr, Mn, Fe, Ni, Cu, Zn, Sr and Pb) were obtained by time (1 h) and size ($PM_{2.5}$ particulate matter <2.5 µm) resolved Particle Induced X-ray Emission (PIXE) measurements. In the Marie Curie FP7-EU framework of SAPUSS (Solving Aerosol Problems by Using Synergistic Strategies), the unique approach used is the simultaneous PIXE measurements at two monitoring sites: urban background (UB) and a street canyon traffic road site (RS). Elements related to primary non exhaust traffic emission (Fe, Cu), dust resuspension (Ca) and anthropogenic Cl were found enhanced at the RS, whereas industrial related trace metals (Zn, Pb, Mn) were found at higher concentrations at the more ventilated UB site. When receptor modelling was performed with positive matrix factorization (PMF), nine different aerosol sources were identified at both sites: three types of regional aerosols (secondary sulphate (S) – 27 %, biomass burning (K) – 5 %, sea salt (Na-Mg) – 17 %), three types of dust aerosols (soil dust (Al-Ti) – 17 %, urban crustal dust (Ca) – 6 %, and primary traffic non exhaust brake dust (Fe-Cu) – 7 %), and three types industrial aerosol plumes-like events (shipping oil combustion (V-Ni) – 17 %, industrial smelters (Zn-Mn) – 3 %, and industrial combustion (Pb-Cl) – 5 %). The validity of the PMF solution of the PIXE data is supported by strong correlations with external single particle mass spectrometry measurements. Beside apportioning the aerosol sources, some important air quality related conclusions can be drawn about the $PM_{2.5}$ fraction simultaneously measured at the UB and RS sites: (1) the regional aerosol sources impact both monitoring sites at similar concentrations regardless their different ventilation conditions; (2) by contrast, local industrial aerosol plumes associated with shipping oil combustion and smelters activities have a higher impact on the more ventilated UB site; (3) a unique source of Pb-Cl (associated with industrial combustion emissions) is found a to be the major (82 %) source of Cl in the urban agglomerate; (4) $PM_{2.5}$ traffic brake dust (Fe-

Cu) is mainly primarily emitted and not resuspended, whereas $PM_{2.5}$ urban crustal dust (Ca) is found mainly resuspended by both traffic vortex and sea breeze; (5) urban dust (Ca) is found the aerosol source most affected by land wetness, reduced by a factor of eight during rainy days and suggesting that wet roads may be a solution for reducing dust concentrations in road sites, far more effective than street sweeping activities.

1 Introduction

It has been largely recognized that air quality and exposure to air pollution have severe consequences and direct growing effects on human health such as diseases of the respiratory and cardiac systems (Dockery et al., 1993; Pope and Dockery, 2006). The effects have become of large interest in urban areas where the population density and human activities are highly concentrated. The sources of $PM_{2.5}$ (PM < 2.5 µm; fine) and $PM_{2.5-10}$ (PM 2.5–10 µm; coarse) usually differ and they include a wide range of natural phenomena and human activities. Typically, the fine particles are produced from combustion processes, forest fires and transformations of gaseous species, whereas coarser ones originate from sea salt, constructions/demolitions, non-exhaust vehicle emissions. Contradicting theories exist as to whether fine or coarse PM produces health effects (Brunekreef and Holgate, 2002; Brunekreef and Forsberg, 2005). However, the size cut at $PM_{2.5}$ does not separate compositions from main different sources well and several studies shows that PM_1 (PM < 1 µm) would be far more effective at separating particles from these sources which produce drastically different compositions (Pastor et al., 2003; Amato et al., 2009a). In other words, the $PM_{0-2.5}$ fraction lying between the PM_{0-1} and the PM_{1-10} ones is the most difficult to characterize as composed of a large variety of aerosol sources. In the European Union, the Clean Air for Europe (CAFE) establishes that an annual limit value of 25 µg m^{-3} must be reached by January 2015 (EEA, 2010). A detailed knowledge of the chemical composition of particles – alongside knowledge of their size and concentration – is important to apportion the sources of PM in the atmosphere. The vast majority of aerosol source

apportionment studies in the literature are limited by the time resolution of the input samples, typically off-line filter collections of 12–24 h (Viana et al., 2008; Pant and Harrison, 2012). However, the impact on PM levels and personal exposure of many sources like industries or vehicular traffic as an emission source is more evident on an hourly time basis. Furthermore, source apportionment receptor models need a series of samples containing material from the same set of sources in differing proportions. Increasing the time resolution of the measurements typically provides samples that have greater between-sample variability in the source contributions than samples integrated over longer time periods.

For this purpose, in this study we performed measurements with the PIXE technique, providing hourly elemental concentrations of the $PM_{2.5}$ aerosol mass loadings. PIXE offers very high sensitivities, thus allowing the use of samplers with high time and size resolution (Lucarelli et al., 2011). This study is part of the SAPUSS project, involving concurrent measurements of aerosols with multiple techniques occurring simultaneously (Dall'Osto et al., 2012a). The aim of the present study is to monitor the elemental concentrations simultaneously measured at a RS and at an UB site during a four-week campaign. The road increments (road concentrations minus urban background concentrations) are investigated as well as other differences found among the two sites. Furthermore, PMF analysis is carried out, and particular emphasis is given in describing the contribution of different sources between the two monitoring sites. Previous work in the same WMB region by using similar techniques focused on PM_{10} trace metals variations in urban areas and regional surrounding (Moreno et al., 2011), on PM_{10} roadside enrichment of atmospheric particulate pollutants (Amato et al., 2011) and on the air quality benefit of street clean activities (Amato et al., 2010). The novelty of this study stands in the analysis on simultaneous $PM_{2.5}$ aerosols data collected at the UB and RS SAPUSS monitoring sites, in the application of PMF receptor modeling to the hourly data in order to apportion different aerosol sources, and in the comparison of such results with the ones obtained by two Aerosol Time-of-Flight Mass Spectrometers (ATOFMSs) during the SAPUSS study. Special emphasis is given in describing all de-

tected elements and their association to regional and local aerosol sources, including different types of road dust and unique anthropogenic plumes of oil combustion, trash burning and industrial activities.

2 Methods

2.1 Location

The SAPUSS campaign (Dall'Osto et al., 2012a) was carried out mainly in Barcelona, a city located in the WMB in the North East (NE) part of Spain. The sampling campaign took part in Barcelona between 20 September and 20 October 2010 (local time, UCT + 2). The unique SAPUSS approach involved a large variety of instrumentation deployed simultaneously in a number of monitoring sites (six), but PIXE analysis was carried out only on the two SAPUSS supersites:

- Road site (RS) was situated in a car park next to C/Urgell. The road, which cuts the city from South East to North West, is a street canyon composed by a two-way cycling path and a one-way four lane vehicle road. Vehicle intensity for the month of measurements was about 17 000 vehicles per day.
- Urban Background site (UB) was situated at the North Western periphery of the city centre in a small park. It is important to note that a main road (Avenida Diagonal, 127 000 vehicles/day) is located about 500 m away from the site.

The two sites were about 2 km away from each other (Dall'Osto et al., 2012a). However, whilst the wind can impact the UB site at all directions, the RS urban street canyons characteristic reduce natural ventilations. In other words, the mechanically generated wind flow and turbulence at the RS are the results of combined processes of atmospheric wind and vehicular traffic.

2.2 Instrumentation

A compact and versatile sampler which collects hourly samples on a unique frame (the two-stages, continuous streaker sampler) was deployed. The sampling devices (Prati et al., 1998) are designed to separate the fine and the coarse modes of an aerosol. A paraffin-coated Kapton foil is used as an impaction surface for coarse particles and a Nuclepore filter as a fine particle collector. The rotation speed of the two collecting plates during sampling, the pumping orifice width and the beam size we use for the subsequent analysis are such that an overall resolution of about 1 h is obtained on the elemental composition of air particulate. PIXE analyses was performed with 3 MeV protons from the 3 MV Tandetron accelerator of the LABEC laboratory of INFN in Florence, with the external beam set-up extensively described elsewhere (Chiari et al., 2005; Calzolai et al., 2006). The beam (30–80 nA) scanned the streak in steps corresponding to 1 h of aerosol sampling; each spot was irradiated for about 180 s. PIXE spectra were fitted using the GUPIX software package and elemental concentrations were obtained via a calibration curve from a set of thin standards of known areal density. The accuracy of hourly elemental concentrations was determined by a sum of independent uncertainties on: standard samples thickness (5 %), aerosol deposition area (2 %), air flow (2 %) and X-rays counting statistics (2–20 %). Detection limits were about 10 ng m^{-3} for low-Z elements and 1 ng m^{-3} for medium-high Z elements. The following elements were detected: Na, Mg, Al, P, S, Cl, K, Ca, Ti, V, Cr, Mn, Fe, Ni, Cu, Zn, Sr and Pb. Unfortunately Nuclepore filters were contaminated by Si and Br whose concentrations was not possible to determine. During SAPUSS, hourly data were collected between 27 September 2010 and 19 October 2010 for a total of 528 h. Data coverage during this period was 80 % at the UB and 57 % at the RS. The overlap between the two sites was higher than 98 %, making 57 % of the time having simultaneous measurements. It is important to note that only the fine $PM_{2.5}$ fraction data analysis is reported in this study.

2.3 Source apportionment method

The source apportionment analysis of the PIXE data was carried out by PMF, and both datasets (UB and RS) were analysed simultaneously. A 506 rows (time; hours) by 17 columns (elements; concentrations) matrix of hourly concentration data was used. To our knowledge, this is the first time such study is attempted. However, it is important to recognise that only the PIXE data are used in this receptor modelling studies, leaving out important components including primary and secondary organic and inorganic species (organic carbon, elemental carbon, secondary inorganic ions, etc.). One advantage of the present study is to test the capability of the hourly PIXE data to capture different aerosol sources. Given the fact that some aerosol sources may show a temporal variation of only few hours, this study may reveal unique aerosol sources not identified with a dataset with a larger variety of chemical species but at lower (daily) time resolution. On the other hand, future SAPUSS receptor modelling studies will focus on combined hourly data obtained from different types of particle mass spectrometers (Dall'Osto et al., 2012a).

The Polissar et al. (1998) procedure was used to choose the data and their associated uncertainties as the PMF input data. PMF solutions from 5 to 10 factors were systematically explored (also changing the FPEAK value) and the resulting *Q* values, the scaled residuals, and the **F** and **G** matrices were examined to find the most reasonable solution. Finally, the solution with nine sources and PEAK = 0 was the most reasonable. The scaled residuals (Paatero and Hopke, 2003) were almost normally distributed and between ±3 for the majority of the species. Finally, it is important to note that the validity of the PMF solution was further supported by correlation with external measurements taken during the SAPUSS, as discussed in Sect. 4.

3 Results

According to earlier studies, the ambient $PM_{2.5}$ concentrations (annual average at urban background: 2003–2006) in Barcelona were in the ranges of 25–29 $\mu g\,m^{-3}$ (Perez et al., 2008), although a reduction has been noticed in the last 2007–2011 period (17–20 $\mu g\,m^{-3}$, Reche et al., 2011) as a result of air quality mitigations and financial crisis. During the SAPUSS, average concentrations of $PM_{2.5}$ were 18.6 $\mu g\,m^{-3}$ and 16.2 $\mu g\,m^{-3}$ at the RS and UB, respectively (Dall'Osto et al., 2012a).

3.1 Overview of $PM_{2.5}$ elements concentrations detected by the PIXE

3.1.1 $PM_{2.5}$ inter comparison between PIXE and off line techniques

Elemental mass concentrations obtained by PIXE were compared to daily filter measurements during SAPUSS. Briefly, $PM_{2.5}$ daily mass concentrations (24 h time resolution) were determined by standard gravimetric procedures and analyzed following the procedures described by Querol et al. (2001): Al, Ca, K, Mg, Fe, Ti, Mn, P, S, Na and 25 trace elements by conventional methods including ion chromatography, inductively coupled plasma atomic emission spectrometry and mass spectrometry (IC, ICP-AES and ICP-MS, respectively Dall'Osto et al., 2012a). Accordingly, the hourly PIXE data were binned into 24-h intervals. Table 1 displays the overall good comparison of filters and PIXE data for the $PM_{2.5}$ mass concentrations. Regression lines (equations in Table 1 with zero intercept set) shows good agreements between PIXE and off line measurements within 5–35 % for Na, Mg, Al, S, K, Mn, Fe, Ni, Cu, Zn and Pb for both UB and RS sites. Some missing data and/or low elemental concentrations did not allow a full intercomparison: Ca and V (also within 30 %) were only available at the RS site. By contrast, limited number of data points and lack of temporal overlaps did not allow comparing Cl, Ti, Cr and Sr at both sites (Table 1). Overall, this study is in line with previous ones, supporting an overall fair correlation between PIXE and off line filters

based techniques as reported in previous studies (Richard et al., 2011; Moreno et al., 2011; Amato et al., 2011).

3.1.2 Average concentrations and site inter comparison

Table 1 presents an overview of the mean elemental concentrations ($\pm 1\sigma$) measured at both UB and RS sites. Average detected $PM_{2.5}$ mass concentration (expressed as sum of the masses of the elements analyzed) for UB and RS was 1.52 $\mu g\,m^{-3}$and 1.64 $\mu g\,m^{-3}$ (respectively), with a slightly higher total concentration (8 %) at the RS. It is therefore important to note that only about 10 % of the total $PM_{2.5}$ mass is apportioned in this study. The remaining mass is due to components not detected by PIXE (elemental carbon, organic carbon, ammonium, nitrate – see Dall'Osto et al., 2012a). Most elements (10 of the monitored 17) did not present statistically significant differences in concentrations between the UB and the RS site (Table 1). Fine S was found the most abundant element ($640 \pm 350\,ng\,m^{-3}$, averaged at both sites), characterized by a time component similar for most of the time at the two sampling sites and typical of secondary aerosols of regional origin; although a spike in concentration was observed on 1 October between 8 p.m. and 12 p.m. only at the UB (Fig. 1). Na was found to be the second most abundant element at both sites at similar concentrations (Table 1). The Mg/Na ratio (0.13 at UB, 0.12 at RS) is typical of bulk sea-water (Mg/Na = 0.12, Seinfeld and Pandis, 1998) and the percentage of Cl depletion was often above 90 %. The sea-salt Sulphur (ss-S) contribution was estimated to be on average 10 % in UB and 14 % in RS during the episodes (with maximum values of about 30 %) and in average below 6 % during the remaining period.

As far as the concentrations of soil related elements are concerned, some elements (Na, Mg, Al, K, Ti) did not present any difference between the two monitoring sites. By contrast, higher concentrations of Ca (17 %), Fe (27 %) and Cu (20 %) were found at the RS relative to the UB. These increments are likely to be due to soil urban dust for Ca, and to non-exhaust primary traffic dust for Fe and Cu (Amato et al., 2011). The temporal patterns of Fe and Cu (Fig. 1) show a periodic behavior with two peaks in

coincidence with the traffic rush hours. Increased attention is focussing on non-exhaust emissions as exhaust emissions are progressively limited by regulations. Denier van der Gon et al. (2007) estimated that 50–75 % of the Cu emissions to the atmosphere in Western Europe are due to brake wear. Several authors (Weckwerth, 2001; Sternbeck et al., 2002; Chellam et al., 2005; Gietl et al., 2010; Amato et al., 2011) also indicated Cu, Fe, Zn, and Ba as candidate marker metals for car non-exhaust.

The elemental ratios of soil related elements revealed different contributions of Al-Ti rich and Ca rich particle types. Previous work also already reported Saharan dust intrusion in South Europe (Chiari et al., 2005; Marenco et al., 2006). Figure 1 shows an increase in concentrations for Al and Ti during the period of 8–10 October (North African air masses, Dall'Osto et al., 2012) simultaneously at the two SAPUSS monitoring sites. This can also be seen in Fig. 2, where the Fe/Ca, Fe/Al, Ca/Al ratios changed from 1.07, 1.88, 2.15 during days affected by marine Polar air masses to 1.44, 0,80, 0.59 during Continental Tropical Saharan episodes (Dall'Osto et al., 2012a). Some trace elements (V, Mn, Ni, Cu, Zn) usually associated to industrial emissions were found to present similar concentrations reported in previous studies (Pey et al., 2009; Amato et al., 2011; Moreno et al., 2011), whereas higher level of Cr and Pb were recorded during the SAPUSS field study (Table 1). Industrial emission related trace elements were found in higher concentrations at the UB site (Pb, Zn and Mn – 42 %, 41 % and 23 %, respectively – Table 1). The increment of Cl at the RS is also related to anthropogenic emissions, although a more in depth discussion is given in the Sect. 3.2. Elevated $PM_{2.5}$ Zn concentrations were previously reported in Barcelona, associated with Pb and attributed to emissions from smelters (Amato et al., 2009b, 2011). Ni was found to be a complex multiple source pollutants, associated to industrial sources including stainless steel and oil combustion ones. V and Ni are usually the most abundant metals present in crude oil (Pacyna and Pacyna, 2001; Moreno et al., 2010; Pandolfi et al., 2011). Since 2007, power plant generators in the Barcelona province are natural gas base, therefore most of the Ni and V sources can be attributed to shipping emissions.

Some consideration on the maximum concentration values of the elements reported in Table 1 are herein made. On average, hourly maximum concentrations values were 2.6 times higher than their daily average values (Table 1). Some metals presented maximum concentrations 3–5 times higher than their average (Ca, Mn, Fe), up to 8–10 (Mn, Zn). Hourly peak concentrations of Zn and Cu analyzed by PIXE can reach maximum hourly levels as high as 506 ng Zn m^{-3} and 345 ng Cu m^{-3} when sampled in regions affected by strong industrial activities (De la Campa, 2011). Our study shows that the urban city of Barcelona can be impacted by industrial plumes of the same order of magnitude for Zn (max value 377 ng Zn m^{-3}).

It is important to note that these events with very high hourly concentrations can shift their total average concentration. Figure S1 in the Supplement shows the frequency distributions of the hourly concentrations for both monitoring sites. When compared to the averages reported in Table 1, indeed lower average concentrations values are found for Gaussian distributions (Fig. S1 in the Supplement) for Na, Ca, Mn and Zn relative to their arithmetic average (Table 1), implying that these four elements are particularly subjected to short temporal events with very high concentrations.

Table 2 shows the R^2 correlation table obtained by comparing the temporal variation of the elemental concentrations simultaneously detected at the UB and RS sites. When the same element is compared between the two sites, some elements represent fairly good correlation: Na (0.63), Mg (0.62), Al (0.43), Cl (0.55), Ca (0.39), Ti (0.40) and Mn (0.51). Sulphur showed a poor correlation (0.33) between the two sites, but when the local UB event of the 1 October was removed, the correlation increased to 0.75. Unexpectedly, other trace metals (V, Cr) usually associated with industrial emissions were found correlating only moderately well at the two sites although some others ones (Pb, Zn, Mn) did present some intra correlations at the two sites (Table 2). The reason is likely to be due to the limited natural ventilation of the RS site (a street canyon, a very typical condition in the urban agglomerate of Barcelona), impeding industrial plumes to disperse in the lower urban surface of the city (Solazzo et al., 2007). Another reason may lie in the fact that the spatial dimension of these industrial plumes may be

smaller than the distance between the two monitoring sites, hence impacting only part of the urban agglomerate. Fe and Cu were not found correlating with any other metals neither among the two different sites because of their local non-exhaust primary traffic emissions source.

3.1.3 Diurnal profiles

Due to the high time resolution of the PIXE data it was possible to detect the average diurnal variation of the elemental mass concentrations, which some are displayed in Fig. 3. The diurnal temporal variation can be influenced by atmospheric mixing and dilution, but also from the mere traffic pattern. Some elements did not present clear diurnal variation, indicating a regional rather than a local origin. For example, S presented similar diurnal profiles at both sites (Fig. 3a) and the divergence in the evening times at UB is due to a local spike event seen on the 1 October. Mg (as well as Na and K) also presented modest variation during the day (Fig. 3b), suggesting additional regional sources (biomass burning and sea salt).

Ca and Al, two common element associated with dust, presented different trends. Ca showed a strong morning peak likely due to traffic (Fig. 3c), but also an additional contribution in the afternoon likely to be due to dust resuspension. By contrast, Al did not show such a marked diurnal variation (Fig. 3d). Both Fe and Cu show a related pattern to the rush-hour times of increased traffic activity during morning (7–9 a.m.) and evening times (6–9 p.m., Fig. 3d–e). Mn, Zn and Pb were mainly seen during night time as industrial plumes impacting the city, probably due both to wind direction and industrial cycles. These seaward overnight industrial plumes are driven by the land breezes channeled along the Llobregat River, which delimits the western side of Barcelona (Pey et al., 2010; Dall'Osto et al., 2012). By contrast, Ni was observed both in the night and in the afternoon when sea breeze brings pollution from the port, as reported in previous studies (Moreno et al., 2011).

3.1.4 Air mass influences

Average concentrations as a function of different air mass for both sites were investigated, in order to see the effect of air masses on the selected elements. Some elements presented more than a 2-fold concentration increase at both sites (relative to average concentration) under specific air masses: Al Ti, K and Fe under North African East (NAF_E) air masses. By contrast, Zn, Pb, Mn, Cl concentrations were found enhanced under Northerly Atlantic air masses (ATL, Dall'Osto et al., 2012a). Other elements did show any clear trends. In summary, the complex spatial and temporal relationship of the elements measured in this study did reveal some interesting pattern, but was not able to sensibly advance the understanding of aerosol source apportionment. For this reason, receptor modelling was applied on the hourly concentrations of the elements measured and the results are presented in the next section.

3.2 Source apportionment by PMF analysis

3.2.1 PMF profiles

PIXE $PM_{2.5}$ aerosol mass data with 1-h resolution were used for source apportionment studies with PMF. Rotational ambiguity was tested by analyzing different FPEAK rotations (0.0 was found the most appropriate), several seeds and values of Q/Q_{exp}. Furthermore, the PMF solution is supported by correlation with external data (Aerosol Time-of-Flight Mass Spectrometry – ATOFMS) presented in the next section. The nine profiles obtained are reported in Fig. 4: the left y-axis displays the fraction of the elemental mass concentration as blue column, whereas the right y-axis shows the fraction of the profile signal of each element (the contribution of one element in all profiles sum up to one and depicted as red squares). Three groups were identified, associated to regional (regional sulphate, sea salt and biomass burning), spikes of anthropogenic activities (industrial emissions, oil combustion, waste incinerator) and three types of dust (non exhaust primary traffic brake dust, soil dust and urban dust).

- *Regional Sulphur: Reg. (S), Fig. 4a, (RS 26 %, UB 29 %)*. This source is characterized by Sulphur and it is likely due to the regional background contribution of sulphates, mainly in the form of ammonium sulphate. This component is attributed to secondary sulphate and aged aerosols, it explains the highest fraction of S mass concentrations (64 %).
- *Aged sea-salt: S.S. (Na-Mg), Fig. 4b, (RS 18 %, UB 15 %)*. Primarily characterized by Na and Mg, the Mg/Na ratio suggests that these two elements originate from the same source and have a marine origin. The lack of Cl in this source indicates that a large fraction of the Cl was depleted. Most of Na (59 %) and Mg (41 %) mass concentrations are described by this factor.
- *Biomass burning: B.B. (K), Fig. 4c, (RS 4 %, UB 6 %)*. This source is characterized by K (56 % of total K signal), with small contribution of Cu. K and S are usually associated with wood combustion. This profile does not show presence of S, but presents an enhancement of Cu and Pb as reported in previous studies (Nriagu and Pacyna, 1988; Schauer et al., 2001; Karanasiou et al., 2009; Richard et al., 2011).
- *Soil dust (Al-Ti), Fig. 4d, (RS 11 %, UB 13 %)*. This source is characterized by Al and Ti with contributions from other crustal elements (K, Ti, Ca, Fe and Mn) as well as Na and Mg. This factor described 68 %, 43 % and 24 % of Al, Ti and Fe, respectively. An increase of this factor was found to occur under North African Tropical air masses and attributed to Saharan dust (Dall'Osto et al., 2012), with average concentrations of $550 \pm 200\,ng\,m^{-3}$ (max values: $1800\,ng\,m^{-3}$). However, it is important to note that this factor was also detected as background concentrations before and after the Saharan dust events, although with much lower concentrations ($110 \pm 65\,ng\,m^{-3}$, max values $393\,ng\,m^{-3}$).
- *Urban Dust (Ca), Fig. 4e, (RS 7 %, UB 6 %)*. This profile is characterized primarily by Ca, and, to a lesser extent, by Al, Ti and Mn. Because of its composition,

this source is related to crustal urban soil dust. This profile describes 65 % of the calcium concentrations detected during SAPUSS. The soil factor found in this study can be due not only to soil but also to other anthropogenic activities such as construction and demolition works. The most important costruction-related activites in term of their contribution to particulate matter concentrations are earth-moving opeations (Muleski et al., 2005). Barmpadimos et al. (2011) reported very high contribution of traffic coarse mode urban ambient concentrations but it was stressed that these numbers are somewhat overestimating the traffic contribution because of lack of information on construction activities around the considered sites. Scarce precipitation limits the cleansing of paved surfaces, and as a result, re-suspension is favored (Amato et al., 2012). Further consideration on the unique effect of precipitation on this source is given in Sect. 4.2.

– *Brake dust (Fe-Cu), Fig. 4g, (RS 9 %, UB 5 %)*. This profile is characterized by Fe and Cu (53 % and 60 % of the total concentrations monitored, respectively). These elements are typical traffic markers. The abrasion of brakes produces particles characterized by high concentrations of Cu, Ba, Zn and Fe (Sanders et al., 2003; Hjortenkrans et al., 2007; Johansson et al., 2008). A contribution from Ca (20 % of the total Ca mass measured) should also be noted, likely to be due to re-suspended dust that had been previously deposited upon the pavement (Kim and Henry, 2000) or from lubricating oil additives (Spencer et al., 2006). This profile was found the only one correlating well (R^2 = 0.7) with Black Carbon (BC), likely due to its primary non exhaust vehicles aerosols nature. Another source of primary traffic non exhaust aerosols are particles released by mechanical abrasion of tyres which are characterized by high concentration of Zn (Sörme et al., 2001; Johansson et al., 2008). In a previous work in Barcelona, Amato et al. (2011) did not show a roadside enrichment for fine aerosol Zn concentrations, but suggested that 15 % of coarse Zn may be attributed to road traffic emissions. This dust (Fe-Cu) profile only explained about 5 % of the Zn variation, and a specific PMF factor related to tyre dust was not found in this study.

– *Industrial smelters (Zn-Mn), Fig. 4g, (RS 3 %, UB 4 %).* This profile is attributed to an industrial source characterized by Zn, Mn and some Pb. These metals were previously attributed to emissions from smelters (Moreno et al., 2011). Amato et al. (2010) also reported a PMF factor with high concentrations of Zn, Pb and Mn and attributed it to industrial emissions, whereas a similar factor was attributed more to local workshops and ateliers in the city of Zurich (Richard et al., 2011).

– *Industrial combustion (Pb-Cl), Fig. 4h, (RS 8 %, UB 3 %)*. This factor is a second type of industrial aerosol emissions characterized by Cl, Pb and some Mn. It is important to note that 82 % of the chloride detected during SAPUSS is described by this PMF profile. Whilst this source was never reported in previous work in this region (Moreno et al., 2011; Amato et al., 2010, 2011), its validity is supported by strong external correlation with hourly measurements taken by aerosol time-of-flight mass spectrometry measurements (ATOFMS, Fig. 5a). Figure 5b shows the positive and negative mass spectra of a particle type detected at both monitoring sites with the ATOFMS (Dall'Osto et al., 2012a). Pb was found to be one of the largest contributors to the positive ion spectrum occurring at *m/z* +206, +207 and +208. Often internally mixed with Pb, Zn ions appear at *m/z* +64. Other peaks in the positive ion spectrum include *m/z* 23 (Na), *m/z* 56 (Fe), *m/z* 39 and 113 (K and K_2Cl). In addition to nitrate (*m/z* −46 NO_2 and *m/z* −62 NO_3), chloride (m/−35 Cl) was one of the most abundant ion in the negative spectra. In general, zinc and lead chlorides have relatively low boiling points and are emitted in the gas phase of high temperature combustion sources such as waste incinerators (Ondov et al., 1998; Hu et al., 2003). Combustion of municipal waste produces submicron particles composed of Zn and Pb as well as numerous other metals (Linak at al., 1993), and relative to nonferrous smelters, such aerosol emissions are enriched in Cl (Tan et al., 2002). Across a wide range of locations, altitudes, and particle chemistry, more than 5 % of single particles contain small amounts of Pb (Murphy et al., 2007). By using an ATOFMS, Zhang et al. (2009) reported three major Pb emission sources: coal combustion, waste incineration and phosphate

industry. A similar Pb-Cl ATOFMS particle type detected during SAPUSS (Fig. 5a, b) was previously associated to a waste incinerator source (Moffet et al., 2008a, b) although other studies in the same area (Mexico city) attributed it to multiple sources, including trash burning (Salcedo et al., 2010; Hodzic et al., 2012). Earlier metallurgical source studies also showed high SO_2 concentrations with Pb-Zn smelter plumes, but our study is in line with the one of Moffet et al. (2008a, b) showing weak correlations observed between this aerosol source and SO_2. By contrast, we found it associated with CO emissions, pointing out to a combustion source and further discussed in the Sect. 4.2.3.

– *Oil combustion (Ni-V), Fig. 4i, (RS 13 %, UB 17 %)*. This source is characterized by elements like V or Ni, tracers for any combustion process of heavy oils (Pacyna, 2001) and small contribution from S. This source may therefore be due to the activities of the port of Barcelona. This profile was found the only one of the nine herein reported correlating with SO_2.

In summary, the nine PMF profiles presented give a much better interpretation of the results respect to the ones obtained looking only at correlations among elements (Sect. 3.1). PMF was able to separate regional and local sources, and further results on abundance, temporal trends, diurnal profiles and site inter comparison of PMF profiles are given in the next section.

3.2.2 Abundance, temporal trends, diurnal profiles and site intercomparison of PMF profiles

Table 3 shows the percentage of the PIXE detected mass explained by the nine sources at the two different monitoring sites as well as the average of the two (TOT). The frequency distributions of the sources (hourly data normalised to reconstructed PIXE mass) are presented in Fig. S2 in the Supplement. The three regional aerosol sources (Reg. (S), S.S. (Na-Mg) and B.B. (K)), did not present much variation between the sites, and overall represented 56 % of the aerosol mass detected by the PIXE. By contrast,

some profiles were enhanced at the RS site (Brake dust (Fe-Cu) and Ind. (Pb-Cl)), whereas higher proportion of Oil (Ni-V) were found at the UB site (Table 3). PMF modelling from daily $PM_{2.5}$ in other WMB sites also identified similar sources but traffic related dust was found mixed with secondary and non exhaust ones, likely due to the low time resolution used hence the impossibility to separate multiple sources (Oliveira et al., 2010; Nicolas et al., 2011). Figure 6 shows the temporal trends of the nine different sources at both sites normalised by the total PIXE mass. It is clear a number of different periods can be seen, including a Saharan dust intrusion (8–10 October) and a regional accumulation one (14–17 October). When the profiles are apportioned to different air masses (Dall'Osto et al., 2012), Table 4 shows – as expected – that Reg. (S) has a higher impact under regional air masses scenarios (42 %), and the least ones under the Atlantic air masses scenarios (17 %). The highest loading of soil dust is under NAF air masses from the East sector (37 %). By contrast NAF West air masses (only one day, 3 October) characterised by strong wind coming from the port areas (230–270°) apportion up to 45 % to Ind. (Ni-V) source. Finally, it is interesting to note that Urban dust (Ca) showed the highest percentages under windy Atlantic air mass scenarios (Table 4) favouring coarse dust resuspension.

The validity of the PMF solution is also supported by the correlations shown in Table 5 among the two different sites. Whilst elements concentrations among sites (Sect. 3.1, Table 2) were not found highly correlated, our receptor modelling study is able to separate local from regional sources quite well. The correlation between Reg. (S) among sites for example is very high (R^2 = 0.88). Other regional sources also show good correlations among the two monitoring sites: Soil dust (Al-Ti) (R^2 = 0.69) and S.S. (Na-Mg) (R^2 = 0.55). By contrast, the Brake dust (Fe-Cu) does not appear correlated with any other profile, due to its local traffic nature. Industrial sources showed weaker correlations among the sites, perhaps due to a number of reasons including RS street canyon characteristics and dimension of aerosol industrial aerosols plumes.

Finally, the diurnal trends of the aerosol profile sources are presented in Fig. 7 for both sites. Whilst there was not a clear diurnal variation for the regional aerosol sources

profile (Fig. 7a–c), the soil dust (Al-Ti) was mainly detected in the morning during the Saharan dust outbreak. The Brake dust (Fe-Cu) source shows two peaks coinciding with rush hours, with the morning one far more pronounced (Fig. 7e). The time trend of this source is well correlated with the vehicles traffic count profile at both sites. Interesting is the behaviour of the crustal source (Dust (Ca), Fig. 7f). The rise in the concentrations at both sites is at morning traffic rush hours, but the concentrations remain high during the day with a pronounced increase in the late afternoon. This implies that whilst dust (Fe-Cu) is related to primary traffic aerosols coming from non exhaust particles, the elements (mainly Ca) in the urban soil source are composed by re-suspended road dust and soil transported by wind or re-suspended by human activities. Re-suspension of dust is function of a number of complex variables such as wind speed, number of cars and speed of cars. Street canyon vortices are generally created by the movement of the wind above the canyon. Cars create turbulence which is a cause of resuspension, although the major cause is likely the shear forces between the tyre and the road surface. Amato et al. (2010) also found a comparable mineral factor with constantly higher concentrations during the day without significant variation within the daylight hours of the day. Oil combustion (Ni-V) presented a minimum in the middle of the day and maxim during the night, pointing to a main contribution from the industrial area but also from the port areas (Fig. 7g). Finally, the two industrial profiles presented complex diurnal profiles, with aerosol plumes impacting the city during both day and night time.

4 Discussion and conclusion

4.1 Intercomparison between ATOFMSs results and hourly PMF PIXE profiles

The ATOFMS provides information on the abundance of different organic and inorganic types of aerosol particles as a function of size with high time resolution at single particle level (Suess and Prather, 1999). ATOFMS can also provide quantitative chem-

ical information if a relative sensitivity factor is applied (Dall'Osto et al., 2006). Two ATOFMS were deployed simultaneously during the SAPUSS field study at the RS (TSI 3800-100, aerodynamic lens) and at the UB (TSI 3800, nozzle/skimmer), respectively. During the SAPUSS, 18 and 14 different particle types were apportioned at the RS and at the UB, respectively 10 of which were found the same at both sites. Most of the particle types were found rich in organic carbon, elemental carbon and nitrate (Dall'Osto et al., 2012b). Giving the fact that the PIXE techniques is able to detect only selected inorganic elements, a complete intercomparison of the two techniques in not straight forward. Most of the PMF profiles obtained from this study did not present significant correlations with the ATOFMS particle types. However, fairly good correlations were obtained with the three regional PIXE PMF profiles (Reg. (S) correlating R^2 = 0.85 with ATOFMS regional EC-K; B.B. (K) correlating R^2 = 0.45 with ATOFMS K-CN and S.S. (Na-K) correlating R^2 = 0.35 with ATOFMS NaCl) at both monitoring sites. Specific ATOFMS particle types detected only at the UB site were found correlating with the PMF PIXE profiles: ATOFMS V-rich shipping oil combustion with PIXE PMF Oil (Ni-V) – R^2 = 0.55 – and ATOFMS dust with PIXE PMF dust (Al-Ti) – R^2 = 0.65. Overall, the strongest correlation (R^2 = 0.86) was found to be between ATOFMS Pb-Cl and PIXE Ind. (Pb-Cl), as already discussed in Sect. 3.1 and Fig. 5.

It is important to note that hourly temporal trends of selected metals can be obtained by querying specific *m/z* ratios in the ATOFMS dataset (Gross et al., 2000). Within this SAPUSS special issue, hourly integrated ATOFMS peak areas of selected *m/z* ratios are evaluated for their suitability in representing metals by comparing them with the metals concentrations presented in this study. Several metals ions revealed a semi-quantitative relationship between ATOFMS peak area and PIXE concentrations, although in some cases comparison of these measurements were poor (Mc Gillcuddy et al., 2012).

4.2 Air quality consideration from the PMF PIXE profiles

4.2.1 Regional particle types

Secondary sulphate (Reg. (S)), which is present in secondary and aged aerosol, explains the highest fraction (RS: 26 %, UB: 29 %) of elemental mass concentration in the fine PM. This factor does not exhibit a clear diurnal variation, indicating a regional rather than a local source. Amongst the sources most difficult to quantify by receptor modelling, and for which emissions inventory data are least reliable, wood smoke stands out as posing particular problems (Pio et al., 2008 ; Harrison et al., 2012). Our receptor modelling study was able to separate a factor which we attribute to biomass burning of regional origin. Ondracek et al. (2011) also found that K and S particles have origin mainly in the long range transport or as a regional background aerosol. Interestingly, the regional contribution of the B.B. (K) factor is further supported by its correlation with the Reg. (S) profile (Table 4). As regard of sea spray, the factor we indentified (S.S. (Na-Mg); RS: 18 % UB: 15 %) suggested a strong depletion in Cl. The weak presence of S in this factor confirms the ATOFMS studies showing that the sea spray detected during SAPUSS was mainly internally mixed with nitrate and not with sulphate (Dall'Osto et al., 2012a). In summary, we find a similar impact of regional aerosol sources on both sites in spite the fact the UB site is far more ventilated than the RS one.

4.2.2 Dust

In urban environments coarse PM_{10} particles tend to be dominated by non-exhaust traffic particles including brake dust and resuspension and wind-blown soil (Thorpe and Harrison, 2008). Amato et al. (2009b) showed that soil (mineral) and brake (road) dust can also apportion 12 % and 8 % (respectively) of the finer $PM_{2.5}$ monitored in the city of Barcelona. The present study was successful at separating different types of dust, attributed to three different sources and altogether representing 25 % of the

elements mass concentrations measured. The temporal trends of soil dust (Al-Ti) particles clearly pointed to a strong Saharan Desert origin, as they were mainly detected during the period of 8–10 October under North African air mass scenarios (Dall'Osto et al., 2012a). However, this particle type was also detected at lower background concentrations during other periods of the SAPUSS field study (Fig. 6). By contrast, the occurrence of urban Dust (Ca) presented a more local origin. A remarkable feature of this particle type is its diurnal trend: a morning increase due to traffic combined with an afternoon one reflecting higher wind speed and contribution from construction activity (Fig. 8). Substantial source of aerosol particles from the road traffic is also the mechanical abrasion of the pavement. These particles typically contain high concentrations of Si, Al, Ca, Mg and Fe. The elevated concentrations of above mentioned elements in the coarse mode of road traffic emissions were observed in many studies (Sternbeck et al., 2002; Thorpe and Harrison, 2007). During this study we were not able to find a specific PMF factor for the mechanical abrasion of the pavement, likely to be mixed within the three different dust types. However, we found a specific Brake dust (Fe-Cu) type which we attribute to non exhaust vehicles emissions. Street geometry and atmospheric circulations can affect the PM_{10} roadside concentrations (Harrison et al., 2004), although previous street canyon studies in Barcelona did not reveal clear wind speed dependence (Amato et al., 2011). A great effort was made in understanding the relationship between wind components, traffic counts and the $PM_{2.5}$ aerosol mass concentrations of the three different dust particles. Unfortunately, the only correlation found was the obvious reduction (dilution) of concentrations at higher wind speed for all three dust particle types. The reasons of the complex relationships between wind components, traffic counts and the dust particles may be due to the finer fraction analysed ($PM_{2.5}$), more dependent to dilution processes rather than resuspension ones as opposed to the coarser PM_{10} fraction. Interestingly, we did not find uniform variations for different dust particle types under rainy conditions. Two time periods were identified as dry days (4-5-6 October, DD, average rain concentration: 0.0 $mm\,h^{-1}$) and rainy days (11-12-13 October, RD, average rain concentration: 0.25 $mm\,h^{-1}$). Wet days (relative to dry days)

were found colder (17 °C vs. 21 °C), windier (4.3 m s^{-1} vs. 2.4 m s^{-1}), cloudier (89 vs. 189 W m^{-2}) and with higher RH (75 % vs. 58 %). Average concentrations were calculated for a number of chemical species for the two different periods. Whilst a DD/RD ratio of 1.4 was found for primary aerosols (BC), a ratio of 3, 4 and 8 was found for the soil dust (Al-Ti), brake dust (Fe-Cu) and urban dust (Ca), respectively. In other words – as expected – resuspended urban dust (Ca) is the particle type most affected by the wetness of the land. Street cleaning by sweeper vehicles and/or water jet cleaning showed a 7–10 % decrease in daily PM_{10} values sampled near roadside sites (Amato et al., 2009c), and this study shows that resuspension dust can be greatly reduced (both by rain wash up and/or road wetting hence limiting resuspension) in wetting roads relative to drier ones.

4.2.3 Anthropogenic industrial plumes and urban Chloride aerosol source

The Iberian Peninsula presents several industrial activities related to refuse incineration and metallurgy (Oliveira et al., 2010; Viana et al., 2006). During SAPUSS, three types of anthropogenic industrial plumes apportioned 23 % of the PIXE elemental mass concentrations. We found a particle type typical of oil combustion sources (Oil (Ni-V)), correlating with SO_2, attributed to shipping oil combustions and already reported in previous studies (Viana et al., 2006; Amato et al., 2009, 2010). Another common sources found was rich in Zn and Mn (Ind. (Zn-Mn)) and attributed to smelters (Viana et al., 2006).

However, a unique particle type was reported for the first time in the Barcelona area, called Ind. (Pb-Cl) and associated with a combustion source. Municipal and hazardous waste incinerator have been shown to emit Pb, Zn and Cl particles (Tan et al., 2002; Walsh et al., 2001; Hu et al., 2003; Chang et al., 2000). For this source, Cl is primarily from the burning of plastic such as polyvinyl chloride and paper, whereas the Pb and Zn can be produced from a variety of sources. We systematically found higher concentrations of aerosol associated with Ind. (Zn-Ni) at the UB site relative to the

RS ones, whereas the opposite trend was found for the Ind. (Pb-Cl) source. Dall'Osto et al. (2012a) reported a detailed analysis of the gaseous concentrations at all different SAPUSS monitoring sites. It was found that the diurnal profile of CO shows a similar trend of NO for most of the monitoring sites, confirming its main traffic source. However, an additional CO spike at 1 p.m. (not associated with NO) was evident only at the RS diurnal cycle, pointing out to a non vehicular combustion localised source. Attributing a specific source to this profile is difficult, although the correlation with CO and not with SO_2 points out to a combustion source unknown at this stage. During night times the two industrial sources (Zn-Mn and Pb-Cl) were often correlated at both monitoring sites, hence likely to be associated with smelters activities. However, the unique spike seen at 1 p.m. at the RS site points out to a local combustion source. On that regard, some considerations should be made on fine particle antimony (Sb), recently suggested as garbage burning tracer (Christian et al., 2010) although Sb is also a main tracer of vehicle brake emissions in cities (Sternbeck et al., 2002; Schauer et al., 2006; Querol et al., 2008; Amato et al., 2009; Hodzic et al., 2012). During our study we did not find a clear association of Sb with this Ind. (Pb-Cl) source. Finally, Li et al. (2012) reported up to 3 ppb HCl in Mexico city, suggesting garbage burning as a major (up to 60 %) source of particulate Chloride. Our study also suggests that Pb-Cl combustion emissions are a major source of fine Cl in the city centre of Barcelona, with maximum concentrations up to 530 ng m^{-3}.

4.3 Conclusion

Hourly-resolved PIXE data were successfully used to determine both the source origin of atmospheric pollutants in urban environments and their contribution to the concentrations of the detected elements. The concentrations of the elements depend on a complex interplay of factors that include local geomorphology, meteorological variations, patterns of road use and specific contributions from industrial hotspots. The detailed chemical database with high time resolution presented in this paper demonstrates in more detail than previous studies the spatial and temporal variability of at-

mospheric element content that is a likely characteristic of Barcelona urban area and offers a deeper insight in source identification. By using PMF analysis, we find a number of local as well as regional sources and natural as well as anthropogenic sources. On a mass basis, the most important isolated factor was found to be associated with secondary sulphate (65 %). This was followed by sea salt (17 %) and shipping oil combustion (15 %). Three types of dust particles were found originating from traffic brake dust, urban crustal dust, soil dust and representing 25 % of the total mass detected. A clear advantage of the high time resolution is the possibility to enable the identifications of sources varying a different hours of the day. This is particularly important for aerosol sources that are more locals (spikes events lasting only few hours) rather than regional contributions (lasting longer periods as more influenced by long range transport or air mass back trajectories type). Quantitative results from this study were also correlated with qualitative single particle mass spectrometry measurements. Urban areas in South Europe are frequently above legislation limits as a result of road dust and favorable climatic conditions for photochemical conditions and dust resuspension. When the whole dataset from the SAPUSS campaign will be available, these data will be useful both to obtain a comprehensive characterization of $PM_{2.5}$ particulate in Barcelona and as a starting point for the PMF analysis of the daily samples. Overall, the PIXE technique applied during the SAPUSS campaign has proven useful in separating different regional aerosol sources, different types of dusts, and different types of industrial plume-like events.

Supplementary material related to this article is available online at: http://www.atmos-chem-phys-discuss.net/12/20135/2012/ acpd-12-20135-2012-supplement.zip.

Acknowledgements. FP7-PEOPLE-2009-IEF, Project number 254773, SAPUSS – Solving Aerosol Problems Using Synergistic Strategies (Marie Curie Actions – Intra European Fellowships. Mr. Manuel Dall'Osto). This study was previously supported by research projects from

the D.G. de Calidad y Evaluacion Ambiental (Spanish Ministry of the Environment) and the Plan Nacional de I+D (Spanish Ministry of Science and Innovation [CGL2010-19464 (VAMOS) and CSD2007-00067 (GRACCIE)]), a collaboration agreement CSIC-JRC, and the Departaments of Medi Ambient from the Generalitat de Catalunya and Diputacio of Barcelona. The University of Birmingham (UK) and the University of Cork (Ireland) SAPUSS ATOFMS teams are also acknowledged.

References

Amato, F., Pandolfi, M., Viana, M., Querol, X., Alastuey, A., and Moreno, T.: Spatial and chemical patterns of PM_{10} in road dust deposited in urban environment, Atmos. Environ., 43, 1650–1659, 2009a.

Amato, F., Pandolfi, M., Escrig, A., Querol, X., Alastuey, A., Pey, J., Perez, N., and Hopke, P. K.: Quantifying road dust resuspension in urban environment by multilinear engine: a comparison with PMF2, Atmos. Environ., 43, 2770–2780, 2009b.

Amato, F., Querol, X., Alastuey, A., Pandolfi, M., Moreno, T., Gracia, J., and Rodriguez, P.: Evaluating urban PM_{10} pollution benefit induced by street cleaning activities, Atmos. Environ., 43, 4472–4480, 2009c.

Amato, F., Nava, S., Lucarelli, F., Querol, X., Alastuey, A., Baldasano, J. M., and Pandolfi, M. A: Comprehensive assessment of PM emissions from paved roads: real-world emission factors and intense street cleaning trials, Sci. Total Environ., 408, 4309–4318, 2010.

Amato, F., Viana, M., Richard, A., Furger, M., Prévôt, A. S. H., Nava, S., Lucarelli, F., Bukowiecki, N., Alastuey, A., Reche, C., Moreno, T., Pandolfi, M., Pey, J., and Querol, X.: Size and time-resolved roadside enrichment of atmospheric particulate pollutants, Atmos. Chem. Phys., 11, 2917–2931, doi:10.5194/acp-11-2917-2011, 2011.

Amato, F., Schaap, M., Denier van der Gon, H. A. C., Pandolfi, M., Alastuey, A., Keuken, M., and Querol, X: Build-up of inhalable road dust particles in Central and Southern Europe, Atmos. Environ. under revision, 2012.

Barmpadimos, I., Nufer, M., Oderbolz, D. C., Keller, J., Aksoyoglu, S., Hueglin, C., Baltensperger, U., and Prévôt, A. S. H.: The weekly cycle of ambient concentrations and traffic emissions of coarse (PM_{10}–$PM_{2.5}$) atmospheric particles, Atmos. Environ., 45, 4580–4590, doi:10.1016/j.atmosenv.2011.05.068, 2011.

Brunekreef, B. and Forsberg, B.: Epidemiological evidence of effects of coarse airborne particles on health, Eur. Respir. J., 26, 309–318, 2005.
Brunekreef, B. and Holgate, S. T.: Air pollution and health, Lancet, 360, 1233–1242, 2002.
Calzolai G., Chiari, M., García Orellana, I., Lucarelli, F., Migliori, A., Nava, S., and Taccetti, F.: The new external beam facility for environmental studies at the Tandetron accelerator of LABE C., Nucl. Instrum. Meth. B, 249, 928–931, 2006.
Chang, M. B., Huang, C. K., Wu, H. T., Lin, J. J., and Chang, S. H.: Characteristics of heavy metals on particles with different sizes from municipal solid waste incineration, J. Hazard. Mater., 79, 229–239, 2000.
Chiari, M., Lucarelli, F., Mazzei, F., Nava, S., Paperetti, L., Prati, P., Valli, G., and Vecchi, R.:Characterization of airborne particulate matter in an industrial district near Florence by PIXE and PESA, X-Ray Spectrom., 34, 323–329, 2005.
Christian, T. J., Yokelson, R. J., Cárdenas, B., Molina, L. T., Engling, G., and Hsu, S.-C.: Trace gas and particle emissions from domestic and industrial biofuel use and garbage burning in central Mexico, Atmos. Chem. Phys., 10, 565–584, doi:10.5194/acp-10-565-2010, 2010.
Dall'Osto, M., Harrison, R. M., Beddows, D. C. S., Freney, E. J., Heal, M. R., and Donovan, R. J.: Single particle detection efficiencies of aerosol time of flight mass spectrometry during the North Atlantic marine boundary layer experiment, Environ. Sci. Technol., 40, 5029–5035, doi:10.1021/es050951i, 2006.
Dall'Osto, M., Querol, X., Alastuey, A., Minguillon, M. C., Alier, M., Amato, F., Brines, M., Cusak, M., Grimalt, J. O., Karanasiou, A., Moreno, T., Pandolfi, M., Pey, J., Reche, C., Ripoll, A., Tauler, R., Van Drooge, B. L., Viana, M., Harrison, R. M., Gietl, J., Beddows, D., Bloss, W., O'Dowd, C., Ceburnis, D., Martucci, G., Ng, S., Worsnop, D., Wenger, J., Mc Gillcuddy, E., Sudou, J., Healy, R., Lucarelli, F., Nava, S., Jimenez, J. L., Gomez Moreno, F., Artinano, B., Prevot, A. S. H., Pfaffenberger, L., Frey, S., Wilsenack, F., Casabona, D., Jiménez-Guerrero, P., Gross, D., and Cotz, N.: Presenting SAPUSS: solving aerosol problem by using synergistic strategies at Barcelona, Spain, Atmos. Chem. Phys. Discuss., 12, 18741–18815, doi:10.5194/acpd-12-18741-2012, 2012a.
Dall'Osto, M, Querol, X., Alastuey, A., Gietl, J., Beddows, D., Roy, M., Harrison, R., Healy, E., Mc Gillcuddy, J., Sudou, J., and Wenger, J.: Simultaneous deployment of single particle mass spectrometry at urban background and road site, SAPUSS special issue, submitted to Atmos. Chem. Phis. Discuss., 2012b.

De la Campa, A. M. S., de la Rosa, J., Gonzalez-Castanedo, Y., Fernandez-Camacho, R., Alastuey, A., Querol, X., Stein, A. F., Ramos, J. L., Rodriguez, S., Orellana, I. G., and Nava, S.: Levels and chemical composition of PM in a city near a large Cu-smelter in Spain, J. Environ. Monitor., 13, 1276–1287, 2011.
Dockery, D. W., Pope III, C. A., Xu, X., Spengler, J. D., Ware, J. H., Fay, M. E., Ferris, B. G., and Speizer, F. E.: An association between air pollution and mortality in six US cities, New Engl. J. Med., 329, 1753–1759, 1993.
EEA: Reporting on Ambient Air Quality Assessment in the EU Member States, 2008ETC/ACC Technical Paper, 2010/11, ETC/ACC, January 2011, 65 pp., 2010.
Gietl, J., Lawrence, R., Thorpe, A. and Harrison, R.: Identification of brake wear particles and derivation of a quantitative tracer for brake dust at a major road., Atmos. Environ., 44, 141–146, 2010.
Gross, D. S., Galli, M. E., Silva, P. J., and Prather, K. A.: Relative sensitivity factors for alkali metal and ammonium cations in single particle aerosol time-of-flight mass spectra, Anal. Chem., 72, 416–422, 2000.
Harrison, R. M., Jones, A. M., and Barrowcliffe, R.: Field study of the influence of metorological factors and traffic volumes upon suspended particle mass at urban roadside sites of differing geometries, Atmos. Environ., 38, 6361–6369, 2004.
Harrison, R. M., Beddows, D. C. S., Hu, L., and Yin, J.: Comparison of methods for evaluation of wood smoke and estimation of UK ambient concentrations, Atmos. Chem. Phys. Discuss., 12, 6805–6838, doi:10.5194/acpd-12-6805-2012, 2012.
Hjortenkrans, D. S. T., Bergbäck, B. G., and Häggerud, A. V.: Metal emissions from brake linings and tires: case studies of Stockholm, Sweden 1995/1998 and 2005, Environ. Sci. Technol. 41, 5224–5230, 2007.
Hodzic, A., Wiedinmyer, C., Salcedo, D., and Jimenez, J. L.: Impact of trash burning on air quality in Mexico City, Environ. Sci. Technol., 1, 4950–4957, 2012.
Hu, C. W., Chao, M. R., Wu, K. Y., Chang-Chien, G. P., Lee, W. J., Chang, L. W., and Lee, W. S.: Characterization of multiple airborne particulate metals in the surroundings of a municipal waste incinerator in Taiwan, Atmos. Environ., 37, 2845–2852, 2003.
Karanasiou, A. A., Siskos, P.A, Eleftheriadis, K.: Assessment of source apportionment by positive matrix factorization analysis on fine and coarse urban aerosol size fraction, Atmos. Environ., 43, 3385–3395, 2009.

Kim B. M. and Henry, R. C.: Extension of self-modeling curve resolution to mixtures of more than three components – Part 3. Atmospheric aerosol data simulation studies, Chemometr. Intell. Lab., 52, 145–154, 2000.

Johansson, Ch., Norman, M., Burman, L.: Road traffic emission factors for heavy metals, Atmos. Environ., 43, 4681–4688, doi:10.1016/j.atmosenv.2008.10.024, 2008.

Li, G., Lei, W., Bei, N., and Molina, L. T.: Contribution of garbage burning to chloride and PM_2.5 in Mexico City, Atmos. Chem. Phys. Discuss., 12, 13667–13689, doi:10.5194/acpd-12-13667-2012, 2012.

Linak, W. P. and Wendt, J. O. L.: Toxic metal emissions from incineration – mechanisms and control, Prog. Energ. Combust., 19, 145–185, 1993.

Lucarelli, F., Nava, S., Calzolai, G., Chiari, M., Udisti, R., and Marino, F.,: Is PIXE still a useful technique for the analysis of atmospheric aerosols? The LABEC experience, X-Ray Spectrom., 40, 4539, 162–167, 2011.

Marenco, F., Bonasoni, P., Calzolari, F., Ceriani, M., Chiari, M., Cristofanelli, P., D'Alessandro, A., Fermo, P., Lucarelli, F., Mazzei, F., Nava, S., Piazzalunga, A., Prati, P., Valli, G., and Vecchi, R.: Characterization of atmospheric aerosols at Monte Cimone, Italy, during summer 2004: source apportionment and transport mechanisms, J. Geophys. Res., 111, D24202, doi:10.1029/2006JD007145, 2006.

Mc Gillcuddy, E., Dall'Osto, M. X., Querol, A., Alastuey, J., Gietl, D., Beddows Roy M., Harrison, R., Healy, J., Sudou, J., Wenger: Hourly quantitative metal concentrations from single particle mass spectrometry, SAPUSS Special Issue, in preparation, Atmos. Chem. Phys. Discuss., 2012.

Moreno, T., Querol, X., Alastuey, A., de la Rosa, J., Sanchez- Campa, A., Minguillon, M., Pandolfi, M., Gonzalez-Castanedo, Y., Monfort, E., and Gibbons, W.: Variations in vanadium, nickel and lanthanoid element concentrations in urban air, Sci. Total Environ., 408, 4569–4579, 2010.

Moreno, T., Querol, X., Alastuey, A., Reche, C., Cusack, M., Amato, F., Pandolfi, M., Pey, J., Richard, A., Prévôt, A. S. H., Furger, M., and Gibbons, W.: Variations in time and space of trace metal aerosol concentrations in urban areas and their surroundings, Atmos. Chem. Phys., 11, 9415–9430, doi:10.5194/acp-11-9415-2011, 2011.

Moffet, R. C., de Foy, B., Molina, L. T., Molina, M. J., and Prather, K. A.: Measurement of ambient aerosols in northern Mexico City by single particle mass spectrometry, Atmos. Chem. Phys., 8, 4499–4516, doi:10.5194/acp-8-4499-2008, 2008a.

Moffet, R. C., Desyaterik, Y., Hopkins, R. J., Tavanski, A. V., Gilles, M. K., Wang, Y., Shutthanandan, V., Molina, L. T., Gonzalez, R., Johnson, K. S., Mugica, V., Molina, M. J., Laskin, A., and Prather, K. A.: Characterization of Aerosols Containing Zn, Pb, and Cl from an, Industrial Region of Mexico City, Environ. Sci. Technol., 42, 7091–7097, 2008b.

Muleski, G. E., Cowherd Jr., C., and Kinsey, J. S.: Particulate emissions from construction activities, JAPCA J. Air Waste Ma., 55, 772–783, 2005.

Murphy, D. M., Hudson, P. K., Cziczo, D. J., Gallavardin, S., Froyd, K. D., Johnston, M. V., Middlebrook, A. M., Reinard, M. S., Thomson, D. S., Thornberry, T., and Wexler, A. S.: Distribution of lead in single atmospheric particles, Atmos. Chem. Phys., 7, 3195–3210, doi:10.5194/acp-7-3195-2007, 2007.

Nicolas, J., Chiari, M., Crespo, J., Galindo, N., Lucarelli, F., Nava, S., and Yubero, E.: Assessment of potential source regions of $PM_{2.5}$ components at a Southwestern Mediterranean site, Tellus B, 63, 96–106, doi:10.1111/j.1600-0889.2010.00510.x, 2011.

Nriagu, J. O. and Pacyna, J. M.: Quantitative assessment of worldwide contamination of air, water and soils by trace metals, Nature, 333, 134–139, 1988.

Ondracek J., Schwarz J., Zdimal V., Andelova L., Vodicka P., Bizek V., Tsai C.-J., Chen S.-C., and Smolik J.: Contribution of the road traffic to air pollution in the Prague City (busy speedway and suburban crossroads), Atmos. Environ., 45, 5090–5100, 2011.

Oliveira, C., Pio, C., Caseiro, A., Santos, P., Nunes, T., Mao, H., Luahana, L., and Sokhi, R.: Road traffic impact on urban atmospheric aerosol loading at Oporto, Portugal, Atmos. Environ., 44, 3147–3158, 2010.

Ondov, J. M. and Wexler, A. S.: Where do particulate toxins reside? An improved paradigm for the structure and dynamics of the urban mid-Atlantic aerosol, Environ. Sci. Technol., 32, 2547–2555, 1998.

Paatero, P. and Hopke, P. K.: Discarding or downweighting high-noise variables in factor analytic models, Anal. Chim. Acta, 490, 277–289, 2003.

Pacyna, J. M. and Pacyna, E. G.: An assessment of global and regional emissions of trace metals to the atmosphere from anthropogenic sources worldwide, Environ. Rev., 9, 269–298, 2001.

Pandolfi, M., Gonzalez-Castanedo, Y., Alastuey, A., de la Rosa, J., Mantilla, E., Sanchez de la Campa, A., Querol, X., Pey, J., Amato, F., and Moreno, T.: Source apportionment o PM_{10} and $PM_{2.5}$ at multiple sites in the strait of Gibraltar by PMF: impact of shipping emissions, Environ. Sci. Pollut. R., 18, 260–269, 2011.

Pant, P. and Harrison, R. M.: Critical review of receptor modelling for particulate matter: a case study of India, Atmos. Environ., 49, 1–12, 2012.

Pastor, S. H., Allen, J. O., Hughes, L. S., Bhave, P., Cass, G. R., and Prather, K. A.: Ambient single particle analysis in Riverside, California by aerosol time-of-flight mass spectrometry during the SCOS97-NARSTO, Atmos. Environ., 37, 239–258, 2003.

Pey, J., Perez, N., Castillo, S., Viana, M., Moreno, T., Pandolfi, M., Lopez-Sebastian, J. M., Alastuey, A., and Querol, X.: Geochemistry of regional background aerosols in the Western Mediterranean, Atmos. Res., 94, 422–435, 2009.

Pey, J., Alastuey, A., and Querol, X.: Discriminating the regional and urban contributions in the North-Western Mediterranean: PM levels and composition, Atmos. Environ. 44, 1587–1596, 2010.

Pio, C. A., Legrand, M., Alves, C. A., Oliveira, T., Afonso, J., Caseiro, A., Puxbaum, H., Sanchez-Ochoa, A., and Gelencser, A.: Chemical composition of atmospheric aerosols during the 2003 summer intense forest fire period, Atmos. Environ., 42, 7530–7543, 2008.

Pope, C. A. and Dockery, D. W.: Health effects offine particulate air pollution: lines that connect, JAPCA J. Air Waste Ma., 56, 709–742, 2006.

Polissar, A. V., Hopke, P. K., Paatero, P., Malm, W. C., and Sisler, J. F.: Atmospheric aerosol over Alaska – Part 2 – Elemental composition and sources, J. Geophys. Res., 103, 19045–19057, 1998.

Prati, P. A., Zucchiatti, S., Tonus, F., Lucarelli, P., Mondo, A., and Ariola, V.: A testing technique of streaker aerosol samplers via PIXE analysis, Nucl. Instrum. Meth. B, 138, 986–989, 1998.

Querol, X., Alastuey, A., Rodriguez, S., Plana, F., Mantilla, E., and Ruiz, C. R.: Monitoring of PM_{10} and $PM_{2.5}$ around primary particulate anthropogenic emission sources. Atmos. Environ., 35, 845–858, 2001.

Querol, X., Pey, J., Minguillón, M. C., Pérez, N., Alastuey, A., Viana, M., Moreno, T., Bernabé, R. M., Blanco, S., Cárdenas, B., Vega, E., Sosa, G., Escalona, S., Ruiz, H., and Artíñano, B.: PM speciation and sources in Mexico during the MILAGRO-2006 Campaign, Atmos. Chem. Phys., 8, 111–128, doi:10.5194/acp-8-111-2008, 2008.

Querol, X., Pey, J., Minguillón, M. C., Pérez, N., Alastuey, A., Viana, M., Moreno, T., Bernabé, R. M., Blanco, S., Cárdenas, B., Vega, E., Sosa, G., Escalona, S., Ruiz, H., and Artíñano, B. New considerations for PM, Black Carbon and particle number concentration for air quality monitoring across different European cities, Atmos. Chem. Phys., 11, 6207–6227, doi:10.5194/acp-11-6207-2011, 2011.

Richard, A., Gianini, M. F. D., Mohr, C., Furger, M., Bukowiecki, N., Minguillón, M. C., Lienemann, P., Flechsig, U., Appel, K., DeCarlo, P. F., Heringa, M. F., Chirico, R., Baltensperger, U., and Prévôt, A. S. H.: Source apportionment of size and time resolved trace elements and organic aerosols from an urban courtyard site in Switzerland, Atmos. Chem. Phys., 11, 8945–8963, doi:10.5194/acp-11-8945-2011, 2011.

Rudnick, R. L. and Gao, S.: Composition of the continental crust, in: Holland HD, Turekian KK, Treatise on Geochemistry, 3, 1–64, 2004.

Salcedo, D., Onasch, T. B., Aiken, A. C., Williams, L. R., de Foy, B., Cubison, M. J., Worsnop, D. R., Molina, L. T., and Jimenez, J. L.: Determination of particulate lead using aerosol mass spectrometry: MILAGRO/MCMA-2006 observations, Atmos. Chem. Phys., 10, 5371–5389, doi:10.5194/acp-10-5371-2010, 2010.

Sanders, P. G., Xu, N., Dalka, T. M., and Maricq, M. M.: Airborne brake wear debris: size distributions, composition, and a comparison of dynamometer and vehicle tests, Environ. Sci. Technol. 37, 4060–4069, 2003.

Schauer, J. J., Kleeman, M. J., Cass, G. R., and Simoneit, B. R.: Measurement of emissions from air pollution sources – 3. C1–C29 organic compounds from fireplace combustion of wood, Environ. Sci. Technol., 35, 1716–1728, 2001.

Schauer, J. J., Lough, G. C., Shafer, M. M., Christensen, W. F., Arndt, M. F., DeMinter, J. T., and Park, J.-S.: Characterization of metals emitted from motor vehicles, Health Effects Institute, Boston, MA, 2006.

Seinfeld J. H. and Pandis S. N.: Atmospheric Chemistry and Physics: From Air Pollution to Climate Change, 1. ed., J. Wiley, New York, 1998.

Solazzo, E., Cai, X., and Vardoulakis, S.: Modelling wind flow and vehicle-induced turbulence in urban streets. Atmos. Environ., 42, 4918–4931, 2008.

Sörme, L., Bergbäck, B., and Lohm, U.: Goods in the anthroposphere as a metal emission source, Water Air Soil Pollut., 1, 213–227, 2001.

Spencer, M. T., Shields, L. G., Sodeman, D. A., Toner, S. M., and Prather, K. A.: Comparison of oil and fuel particle chemical signatures with particle emissions from heavy and light duty vehicles, Atmos. Environ., 40, 5224–5235, 2006.

Sternbeck, J., Sjödin, Â., and Andréasson, K.: Metal emissions from road traffic and the influence of resuspension. A results from two tunnel studies, Atmos. Environ., 36, 4735–4744, 2002.

Suess, D. T. and Prather, K. A.: Mass spectrometry of aerosols, Chem. Rev., 99, 3007–3035, 1999.

Tan, P. V., Fila, M. S., and Evans, G. J., Jervis, R. E.: Aerosol laser ablation mass spectrometry of suspended powders from PM sources and its implications to receptor modeling, JAPCA J. Air Waste Ma., 52, 27–40, 2002.

Thorpe, A. J. and Harrison, R. M.: Sources and properties of non-exhaust particulate matter fromroad traffic: a review, Sci. Total Environ., 400, 270–282, 2008.

Viana, M. M., Querol, X., Alastuey, A., Ibarguchi, J. I., and Menendez, M.: Identification of PM sources by principal component analysis (PCA) coupled with meteorological data, Chemosphere, 65, 2411–2418, 2006.

Viana, M., Kuhlbusch, T. A. J., Querol, X., Alastuey, A., Harrison, R. M., Hopke, P. K., Winiwarter, W., Vallius, M.: Source apportionment of particulate matter in Europe: a review of methods and results, J. Aerosol Sci., 39, 827–849, 2008.

Walsh, D. C., Chillrud, S. N., Simpson, H. J., and Bopp, R. F.: Refuse incinerator particulate emissions and combustion residues for New York City during the 20th century, Environ. Sci. Technol., 35, 2441–2447, 2001.

Zhang, Y. P., Wang, X. F., Chen, H., Yang, X., Chen, J.M., Allen, J. O.: Source apportionment of lead containing aerosol particles in Shanghai using single particle mass spectrometry, Chemosphere, 74, 501–507, doi:10.1016/j.chemosphere.2008.10.004, 2009

Table 1. Intercomparison between PIXE and off-line techniques; average hourly elemental concentrations and minimum and maximum hourly and daily values for the elemements detected by PIXE during the SAPUSS field study (N.A. Not available due to limited number of points).

Element	Inter comparison with off-line techniques		Average Hourly concentrations [ng m^{-3}]			Maximum and minimum values (H = hourly; D = daily)	
	UB	RS	UB	RS	diff RS – UB (%)	UB	RS
Na	$Y = 0.85$ ($R^2 = 0.44$)	$Y = 1.1$ ($R^2 = 0.41$)	430 ± 160	400 ± 220	Not. Sign.	$(32–1016)_H$ $(130–612)_D$	$(68–1295)_H$ $(154–490)_D$
Mg	$Y = 0.78$ ($R^2 = 0.55$)	$Y = 1.25$ ($R^2 = 0.8$)	43 ±16	47 ± 23	Not. Sign.	$(22–106)_H$ $(29–81)_D$	$(24–143)_H$ $(32–68)_D$
Al	$Y = 0.88$ ($R^2 = 0.87$)	$Y = 0.70$ ($R^2 = 0.45$)	50 ± 24	45 ± 30	Not. Sign.	$(15–146)_H$ $(41–130)_D$	$(2.3–181)_H$ $(34–64)_D$
S	$Y = 0.80$ ($R^2 = 0.91$)	$Y = 0.80$ ($R^2 = 0.88$)	669 ± 460	620 ± 320	Not. Sign.	$(103–)_H$ $(308–1230)_D$	$(116–1607)_H$ $(236–882)_D$
Cl	N.A.	N.A.	50 ± 34	71 ± 79	29	$(17–304)_H$ $(19–59)_D$	$(2.5–532)_H$ $(39–91)_D$
K	$Y = 0.85$ ($R^2 = 0.30$)	$Y = 0.81$ ($R^2 = 0.6$)	89 ± 39	82 ± 30	Not. Sign.	$(25–214)_H$ $(54–201)_D$	$(20–178)_H$ $(56–102)_D$
Ca	N.A.	$Y = 1.15$ ($R^2 = 0.60$)	109 ± 86	130 ± 149	17	$(25–665)_H$ $(53–126)_D$	$(21–817)_H$ $(43–294)_D$
Ti	N.A.	N.A.	11 ± 3	12 ± 4	Not. Sign.	$(8.1–23)_H$ $(20–20)_D$	$(8.0–29)_H$ $(8.0–13)_D$
V	N.A.	$Y = 0.80$ ($R^2 = 0.20$)	9 ± 3	8 ± 3	Not. Sign.	$(5.6–17)_H$ $(7.0–13)_D$	$(5.5–16)_H$ $(6.1–10)_D$
Cr	N.A.	N.A.	8 ± 2	8 ± 2	Not. Sign.	$(3.8–16)_H$ $(4.0–12)_D$	$(3.8–16)_H$ $(4.7–10)_D$
Mn	$Y = 1.35$ ($R^2 = 0.40$)	$Y = 1.2$ ($R^2 = 0.55$)	7 ±7	6 ± 5	−23	$(2.5–51)_H$ $(4.0–9.0)_D$	$(2.5–27)_H$ $(3.1–7.2)_D$
Fe	$Y = 1.2$ ($R^2 = 0.7$)	$Y = 0.90$ ($R^2 = 0.7$)	96 ± 60	131 ± 94	27	$(2.2–303)_H$ $(43–155)_D$	$(15–525)_H$ $(54–171)_D$
Ni	$Y = 0.82$ ($R^2 = 0.4$)	$Y = 0.89$ ($R^2 = 0.7$)	3 ± 1	3 ± 1	Not. Sign.	$(1.1–7.6)_H$ $(2.0–5.0)_D$	$(1.0–7.1)_H$ $(1.6–4.2)_D$
Cu	$Y = 0.90$ ($R^2 = 0.65$)	$Y = 0.80$ ($R^2 = 0.7$)	5 ± 3	8 ± 4	20	$(1.2–16)_H$ $(2.0–8.0)_D$	$(1.7–22)_H$ $(2.9–7.5)_D$
Zn	$Y = 0.7$ ($R^2 = 0.65$)	$Y = 0.75$ ($R^2 = 0.75$)	35 ±56	25 ± 31	−41	$(2.8–377)_H$ $(19–55)_D$	$(2.6–249)_H$ $(6.3–57)_D$
Sr	N.A.	N.A.	2 ±1	2 ± 1	Not. Sign.	$(1.4–4.0)_H$ $(1.6–3.0)_D$	$(1.4–3.0)_H$ $(1.4–2.2)_D$
Pb	$Y = 0.85$ ($R^2 = 0.40$)	$Y = 0.95$ ($R^2 = 0.80$)	17 ± 9	12 ± 5	−42	$(4.0–41)_H$ $(3.4–14)_D$	$(4.5–18)_H$ $(5.7–12)_D$

Table 2. Inter-site correlation table (R^2) of the 17 elements simultaneously detected at the UB and RS site. Poor correlations ($R^2 < 0.30$) are not reported for clarity. Intra-site correlations were generally poor and two additional tables were not found useful and space consuming. Intra-site correlations were found generally poor, with only selected elements correlating within each other: Na, Mg ($R^2 = 0.6$); Fe, Cu ($R^2 = 0.7$); Zn, Cl, Pb, Cl ($R^2 = 0.6$); Al, Ti ($R^2 = 0.45$); K, S ($R^2 = 0.4$) and Ni, V ($R^2 = 0.5$).

R^2		Urban background (UB)																
		Na	Mg	Al	S	Cl	K	Ca	Ti	V	Cr	Mn	Fe	Ni	Cu	Zn	Sr	Pb
	Na	0.62	0.4	–	–	–	–	–	–	–	–	0.33	–	–	–	–	–	–
	Mg	0.63	0.52	0.39	–	–	–	–	–	–	–	–	–	–	–	–	–	–
	Al	0.38	0.43	0.43	–	–	0.23	–	–	–	–	–	–	–	–	–	–	–
	S	–	–	–	0.33 (0.75)	–	–	–	–	–	–	–		–	–	–	–	–
	Cl	0.27	–	–	–	0.55	–	–	–	–	–	–	0.26	–	–	0.27	–	0.25
	K	0.39	0.37	0.45	–	–	–	–	–	–	–	–	–	–	–	–	–	–
Road	Ca	–	–		–	–	–	0.39	–	–	–	–	–	–	–	–	–	–
site	Ti	–	0.41	0.61	–	–	0.34	–	0.4	–	–	–	–	–	–	–	–	–
(RS)	V	–	–	–	–	–	–	–	–	–	–	–	–	–	–	–	–	–
	Cr	–	–	–	–	–	–	–	–	–	–		–	–	–	–	–	–
	Mn	–	–	–	–	–	–	–	–	–	–	0.51	–	–	–	–	–	–
	Fe	–	0.23	–	–	–	–	–	–	–	–	–	–		–	–	–	–
	Ni	–	–	–	–	–	–	–	–	–	–	–	–	0.2	–	–	–	–
	Cu	–	–	–	–	–	–	–	–	–	–	–	–	–	–	–	–	–
	Zn	–	–	–	–	–	–	–		–		0.44	–	–	–	–	–	–
	Sr	0.4	0.3	–	–	–	–	–	0.26	0.39	0.35	–	–	–	–	–	–	–
	Pb	–	–	–	–	0.36	–	–	–	–	–	0.58	–	–	–	0.46	–	0.3

Table 3. Percentages (%, sum of the masses of the elements analysed) of the nine PMF profiles at the UB, RS and average UB-RS (TOT) sites.

Class	PMF profile name	TOTAL (UB + RS)	UB	RS
Regional	Reg (S)	27 %	29 %	26 %
	S.S. (Na-Mg)	17 %	15 %	18 %
	B.B. (K)	5 %	6 %	4 %
Dust	Dust (Fe-Cu)	7 %	5 %	9 %
	Dust (Ca)	6 %	6 %	7 %
	Dust (Al-Ti)	12 %	13 %	11 %
Plumes	Ind. (Pb-Cl)	5 %	3 %	8 %
	Ind. (Zn-Mn)	3 %	4 %	3 %
	Oil (Ni-V)	15 %	17 %	13 %
TOTAL		100 %	100 %	100 %

Table 4. Abundance of the PIXE total mass (%) of the nine PMF profiles for different air mass scenarios.

	Reg. (S)	Ind (Pb-Cl)	Dust (Fe-Cu)	B.B. (K)	Ind (Zn-Mn)	S.S. (Na-Mg)	Dust (Al-Ti)	Oil (V-Ni)	Dust (Ca)
Regional (REG)	**42**	5	8	6	4	7	8	16	4
Atlantic (ATL)	17	**10**	9	3	**5**	21	8	14	**11**
North African East (NAF_E)	19	2	4	3	0	22	**37**	10	3
North African West (NAF_W)	23	0	1	5	1	11	11	**45**	3

Table 5. Correlation table (R^2) of the nine PMF profile simultaneously detected at the UB and RS site. Poor correlations ($R^2 < 0.3$) are not reported for clarity.

		RS Reg (S)	RS Ind (Pb-Cl)	RS Dust (Fe-Cu)	RS B.B. (K)	RS Ind (Zn-Mn)	RS S.S. (Na-Mg)	RS Dust (Al-Ti)	RS Oil (Ni-V)	RS Dust (Ca)
UB	Reg (S)	0.88	–	–	0.52	–	–	–	–	–
	Ind (Pb-Cl)	–	0.51	–	–	–	–	–	–	–
	Traf (Fe-Cu)	–	–	0	–	–	–	–	–	–
	B.B. (K)	0.27	–	–	0.35	–	–	–	–	–
	Ind (Zn-Mn)	–	0.27	–	–	0.25	–	–	–	–
	S.S. (Na-Mg)	–	–	–	–	–	0.55	–	–	–
	Dust (Al-Ti)	–	–	–	–	–	–	0.69	–	–
	Oil (Ni-V)	–	–	–	–	–	–	–	0.37	–
	Dust (Ca)	–	–	–	–	–	–	–	–	0.39

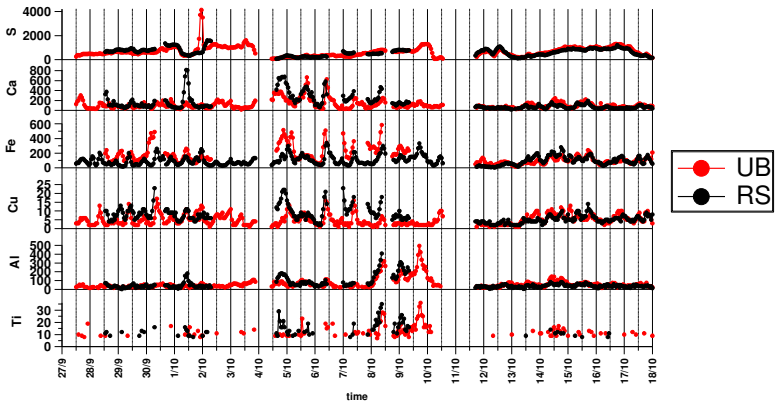

Fig. 1. Temporal trends (all in ng m^{-3}) of selected elements measured simultaneously at the UB and RS sites.

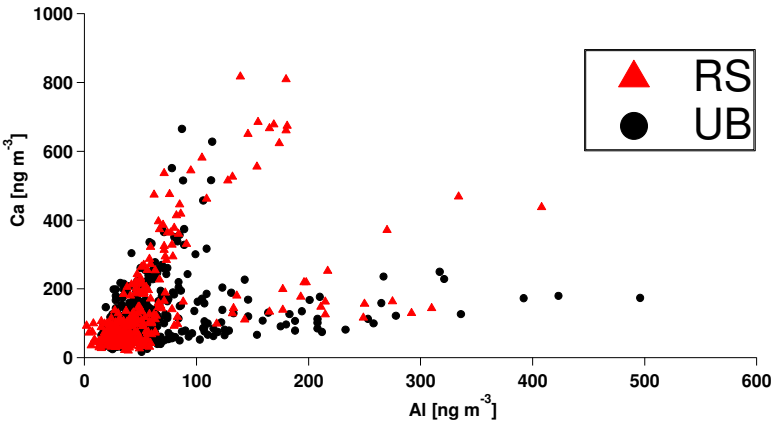

Fig. 2. Ca versus Al concentrations measured at the UB and RS site. Please note the lower ensemble of points is due to the Saharan dust intrusion.

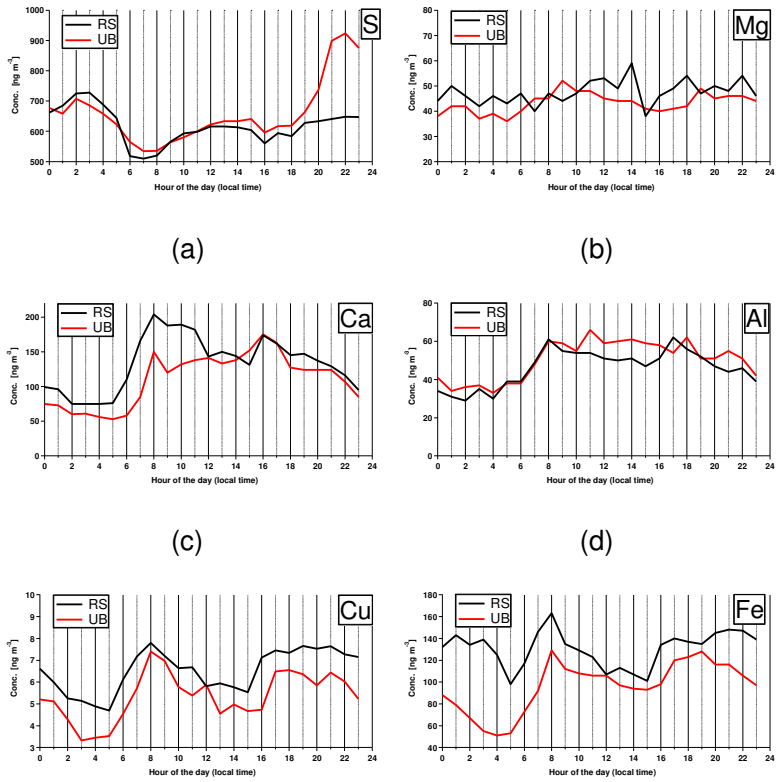

Fig. 3. Diurnal profile of selected elements at the UB and RS site.

Main aerosol class	PMF profile name	Factor profile
Regional	***(a)*** Reg (S)	
	(b) S.S. (Na-Mg)	
	(c) B.B. (K)	
Dust	***(d)*** Dust (Al-Ti)	
	(e) Dust (Ca)	
	(f) Dust (Fe-Cu)	
Antr. Spikes	***(g)*** Ind. (Zn-Mn)	
	(h) Ind. (Pb-Cl)	
	(i) Oil (Ni-V)	

Fig. 4. PMF factor profiles. Average source contributions to elemental concentrations, in ng m^{-3} (left axis – blue columns) and in % of measured elemental concentrations (right axis – red points).

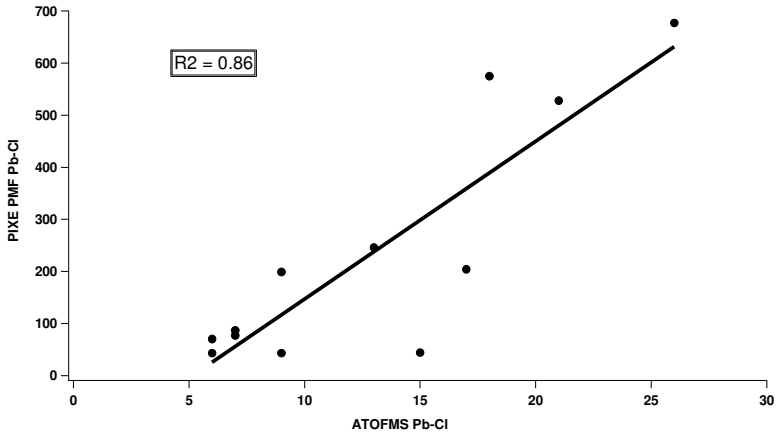

Fig. 5a. Temporal hourly correlation between the PMF factor profile Ind. (Pb-Cl) and an ATOFMS particle type (Pb-Cl), see Dall'Osto et al. (2012a). Please note only ATOFMS counts higher than 5 particles/hour are considered.

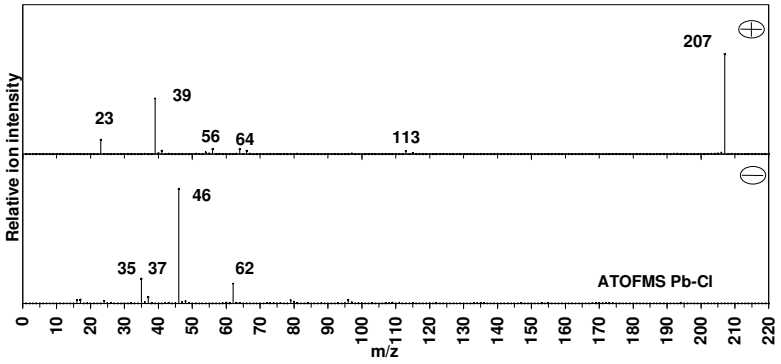

Fig. 5b. Average positive and negative mass spectra of particle type Pb-Cl detected at the RS site by single particle aerosol mass spectrometry (ATOFMS).

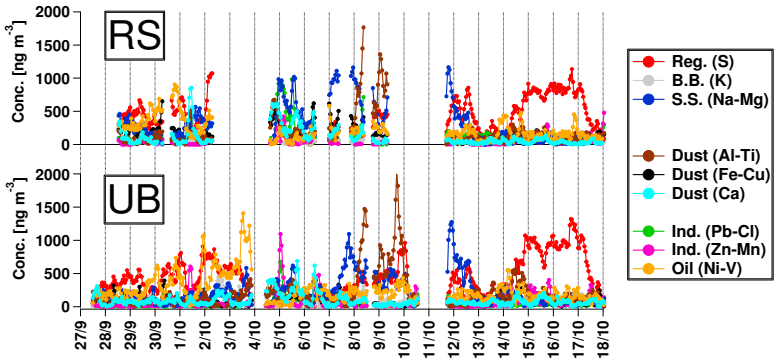

Fig. 6. Temporal trends of the nine PMF factors detected simultaneously at the UB and RS site.

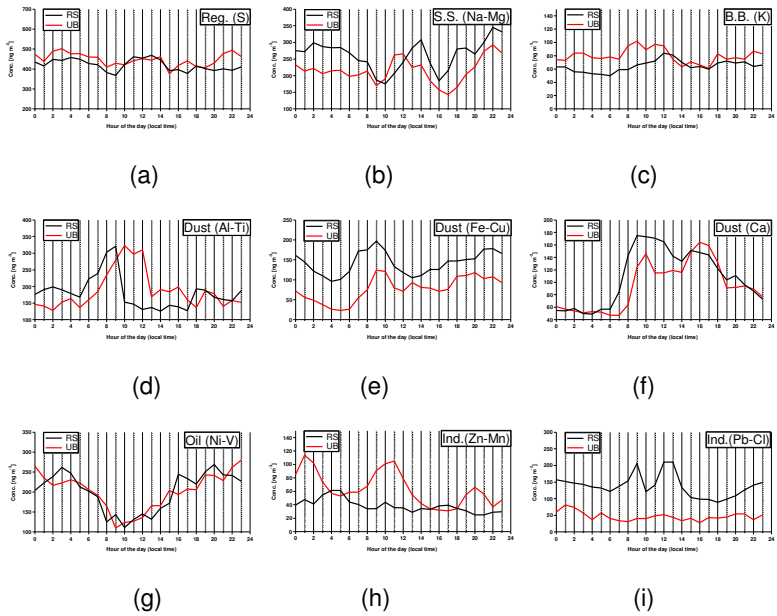

Fig. 7. Diurnal profile of the PMF factors at the UB and RS site.